

# Theoretical Study of Alternative Pathways for the Heck Reaction through Dipalladium and “Ligand-Free” Palladium Intermediates

Panida Surawatanawong and Michael B. Hall\*

Department of Chemistry, Texas A&M University, College Station, Texas 77843-3255

Received August 14, 2008

The pathways for the Heck reaction, in particular, carbon–carbon bond formation between ethylene and phenyl bromide, catalyzed by dipalladium intermediates and substrate-bound palladium complexes, were investigated by density functional calculation. For the sterically hindered phosphine ligand,  $P^tBu_3$ , the free energy barrier for phenyl bromide oxidative addition to  $Pd_2(P^tBu_3)_2$  is significantly higher than that to  $Pd(P^tBu_3)$  due to the higher steric interaction. However, for the  $PMe_3$  ligand, phenyl bromide oxidative addition by  $Pd_2(PMe_3)_2$  has a lower free energy barrier than that by  $Pd(PMe_3)$ . Although the dipalladium is less likely to be active when coordinated by two sterically hindered phosphines, such as  $P^tBu_3$ , it could serve as the active catalyst when less sterically encumbered. For  $Pd_2(PMe_3)_2$ , the free energy profile for the complete Heck reaction cycle shows that, like the monopalladium pathway, oxidative addition of phenyl bromide is the rate-limiting step. Substrate-bound palladium complexes were also investigated as models for “ligand-free” conditions. Of the substrate-bound palladium complexes examined—free  $Pd$ ,  $PdBr^-$ , and  $Pd(\eta^2-C_2H_4)$ —the olefin-coordinated intermediate has the lowest free energy barrier for the phenyl bromide oxidative addition. Examination of the complete Heck reaction cycle for  $PdBr^-$ - and  $Pd(\eta^2-C_2H_4)$ -based intermediates shows that ethylene stabilizes atomic palladium, which then proceeds to oxidative addition and migratory insertion. After the C–C bond coupling, a second bromide or other ligand binds to stabilize the low-coordinated palladium complex before it proceeds to  $\beta$ -H transfer/olefin elimination and catalyst recovery.

## Introduction

The Heck reaction is the palladium-catalyzed arylation reaction of an aryl halide and olefin to form a new C–C bond under basic conditions. A number of ligands, especially phosphine ligands, have been developed to stabilize the palladium catalysts. Recently, a “ligand-free” palladium system has attracted considerable attention.<sup>1–7</sup> Reetz<sup>6</sup> and de Vries<sup>4,6</sup> proposed that the Pd nanoparticles observed in the ligand-free system are the reservoir for the active  $Pd(0)$  catalyst for the Heck reaction. The key success of these systems is to stabilize the palladium colloids to prevent the agglomeration and precipitation of palladium black, which terminates the reaction. Without phosphine ligands, additives such as tetraalkylammonium halides are used to decelerate palladium black formation<sup>2</sup> and to stabilize the Pd colloid,<sup>8</sup> which slowly releases the molecular palladium active species. Increasing substrate to catalyst ratio was also shown to enhance the turnover frequency and to prevent palladium black formation because additional substrate shifts the

equilibrium from palladium nanoparticles to catalytically active palladium molecules.<sup>3,9,10</sup>

During the course of the reaction under the “ligand-free” conditions studied by de Vries and co-workers, dipalladium intermediates with bridging iodides were detected and isolated.<sup>4</sup> Furthermore, several other studies have shown that dipalladium complexes can be catalysts in cross-coupling reactions. Hartwig and co-workers used  $Pd_2(\mu-Br)_2(P^tBu_3)_2$  as the catalyst for Suzuki couplings and amination reactions.<sup>11</sup> In their comparison of two catalysts, (1)  $Pd[P(o-Tol)_3]_2$ , the monopalladium complex, and (2)  $[Pd(P(o-Tol)_3)(Ar)(Br)]_2$  ( $Ar = aryl$ ), the dipalladium intermediate from the aryl halide oxidative addition, Herrmann and co-workers found that both mono- and dipalladium species gave similar results as catalysts for the Heck reaction.<sup>12</sup>

A number of theoretical studies on the Heck reaction mechanism, particularly the oxidative-addition step, have been reported.<sup>13–21</sup> Close attention has been paid to mechanisms

\* Corresponding author. E-mail: mbhall@tamu.edu.

- (1) Reetz, M. T.; Westermann, E. *Angew. Chem., Int. Ed.* **2000**, *39*, 165–168.
- (2) Vries, A. H. M. d.; Parlevliet, F. J.; Vondervoort, L. S.-v. d.; Mommers, J. H. M.; Henderickx, H. J. W.; Walet, M. A. M.; Vries, J. G. d. *Adv. Synth. Catal.* **2002**, *344*, 996–1002.
- (3) Vries, A. H. M. d.; Mulders, J. M. C. A.; Mommers, J. H. M.; Henderickx, H. J. W.; Vries, J. G. d. *Org. Lett.* **2003**, *5*, 3285–3288.
- (4) Vries, J. G. d. *Dalton Trans.* **2006**, 421–429.
- (5) Kohler, K.; Kleist, W.; Prockl, S. S. *Inorg. Chem.* **2007**, *46*, 1876–83.
- (6) Reetz, M. T.; Vries, J. G. d. *Chem. Commun.* **2004**, 1559–1563.
- (7) Schmidt, A. F.; Smirnov, V. V. *J. Mol. Catal. A: Chem.* **2003**, *203*, 75–78.
- (8) Jeffery, T. *Tetrahedron Lett.* **1985**, *26*, 2667–2670.

- (9) Reetz, M. T.; Westermann, E.; Lohmer, R.; Lohmer, G. *Tetrahedron Lett.* **1998**, *39*, 8449–8452.
- (10) Beletskaya, I. P.; Cheprakov, A. V. *Chem. Rev.* **2000**, *100*, 3009–3066.
- (11) Stambuli, J. P.; Buhl, M.; Hartwig, J. F. *J. Am. Chem. Soc.* **2002**, *124*, 9346–9347.
- (12) Böhm, V. P. W.; Herrmann, W. A. *Chem.–Eur. J.* **2001**, *7*, 4191–4197.
- (13) Lin, B.-L.; Liu, L.; Fu, Y.; Luo, S.-W.; Chen, Q.; Guo, Q.-X. *Organometallics* **2004**, *23*, 2114–2123.
- (14) Albert, K.; Gisdakis, P.; Rösch, N. *Organometallics* **1998**, *17*, 1608–1616.
- (15) Ariafard, A.; Lin, Z. *Organometallics* **2006**, *25*, 4030–4033.
- (16) Ahlquist, M.; Norrby, P.-O. *Organometallics* **2007**, *26*, 550–553.
- (17) Ahlquist, M.; Fristrup, P.; Tanner, D.; Norrby, P.-O. *Organometallics* **2006**, *25*, 2066–2073.
- (18) Senn, H. M.; Ziegler, T. *Organometallics* **2004**, *23*, 2980–2988.

involving palladium stabilized by phosphine or carbene ligands. Recently, we examined competitive pathways involving the palladium phosphine complexes as catalysts in the Heck reaction and found that the monophosphinopalladium complex is the most favorable in comparison to diphosphinopalladium and ethylene-bound monophosphinopalladium for the oxidative addition of phenyl bromide, the rate-determining step in our study.<sup>22</sup> Recent experimental results on “ligand-free” palladium systems and on dipalladium complexes increased our interest in alternative mechanisms, as the palladium monophosphine that we studied can form the dipalladium,  $\text{Pd}_2(\text{PR}_3)_2$ , which could be an active catalyst in an alternative Heck reaction mechanism. Furthermore, under “ligand-free” conditions, substrate-bound palladium complexes could play a role as the active species. A recent theoretical study by Ahlquist et al. suggested that alkynes can serve as ligands for the oxidative-addition step in the hydroarylation reaction under phosphine-free conditions.<sup>23,24</sup> Likewise, the olefin substrate might serve as a ligand in the “ligand-free” Heck reaction. Here, we report computational investigations of alternative pathways for the Heck reaction via dipalladium,  $\text{Pd}_2(\text{PR}_3)_2$ , and substrate-bound palladium intermediates—free Pd,  $\text{PdBr}^-$ , and  $\text{Pd}(\eta^2\text{-C}_2\text{H}_4)$ —in comparison to mononuclear palladium phosphine,  $\text{Pd}(\text{PR}_3)$ . These density functional theory (DFT) computations, which include both thermal and solvent corrections, should help elucidate the relative importance of alternative pathways for the Heck reactions.

### Computational Details

All calculations were performed with Gaussian03 program packages.<sup>25</sup> The density functional PBE<sup>26</sup> was used for geometry optimization with the modified LANL2DZ+f basis set for Pd, LANL2DZdp for P and Br atoms with effective core potentials (ECP),<sup>27–29</sup> and 6-31++G(d',p')<sup>30–32</sup> for C, N, and H atoms except for those on the tertiary butyl, where we use 6-31G(d).<sup>30–32</sup> Geometry and frequency calculations were performed with the PBE functional because the density fitting procedure available in pure functionals increases the speed of these calculations. Previous work<sup>33</sup> has shown that the B3LYP energies are similar

**Table 1. Relative B3LYP/PBE Enthalpy and Free Energy of Ligand/Substrate (L) Binding in the Reaction  $\text{Pd}_4 + \text{L} \rightarrow \text{Pd}_3 + \text{PdL}$**

|           |  | $\Delta H$   | $\Delta G_{\text{gas}}$ (1 atm) | $\Delta G_{\text{tot}}$ (1 M) |
|-----------|--|--------------|---------------------------------|-------------------------------|
|           |  | Pd Ligand    |                                 |                               |
| <b>6m</b> | $\text{Pd}(\text{PMe}_3)$                | 2.26         | 2.02                            | −0.39                         |
| <b>6t</b> | $\text{Pd}(\text{P}^t\text{Bu}_3)$       | 2.03         | 2.20                            | −0.70                         |
|           |  | Pd Substrate |                                 |                               |
| <b>32</b> | $\text{Pd}(\eta^2\text{-C}_2\text{H}_4)$ | 10.07        | 9.12                            | 3.06                          |
| <b>41</b> | $\text{Pd}(\eta^2\text{-PhBr})$          | 22.41        | 21.50                           | 17.08                         |
| <b>60</b> | $\text{PdBr}^-$                          | 18.39        | 15.14                           | 19.28                         |

to CCSD(T) energies for  $\text{CH}_4$  oxidative addition to Pd. Our own test calculations showed less than 1 kcal/mol between B3LYP//PBE and all B3LYP calculations for the oxidative addition of phenyl bromide to  $\text{Pd}(\text{PH}_3)_2$  and  $\text{Pd}(\text{PH}_3)$ . Therefore, single-point energies were recalculated with the B3LYP functional<sup>34,35</sup> using the same basis set. All structures were fully optimized with default convergence criteria, and frequencies were calculated to ensure that there are no imaginary frequencies for minima and only one imaginary frequency for transition states. Zero-point energies and thermodynamic functions were calculated at 298.15 K and 1 atm. The solvation energies were calculated on the geometries from PBE gas-phase optimizations by using the CPCM<sup>36,37</sup> method with UAKS atomic radii and solvation parameters corresponding to DMSO ( $\epsilon = 46.7$ ). With the CPCM method and UAKS atomic radii, test calculation of the solvation free energy of  $\text{CH}_3\text{NH}_3$  and *N*-methylacetamide, for which the experimental<sup>38</sup> solvation energies are available, gave an error of less than 1 kcal/mol. The standard states were corrected to 1 mol/L (see Supporting Information for standard state conversion). The energies and structural parameters of some models related to palladium monophosphine with the  $\text{PMe}_3$  ligand were previously published,<sup>22</sup> but some of these results are shown here for comparison.

### Results and Discussion

The observed aggregation of palladium and of the dipalladium intermediates in the Heck reaction led to our interest in a reaction cycle based on dipalladium,  $\text{Pd}_2(\text{PR}_3)_2$ , as the active catalyst. The success of low-loading palladium in “ligand-free” conditions also prompted us to investigate reaction pathways involving phosphine-free substrate-bound palladium intermediates: free Pd,  $\text{PdBr}^-$ , and  $\text{Pd}(\eta^2\text{-C}_2\text{H}_4)$ . Generally, the following steps were examined: the oxidative addition of the phenyl bromide, the migratory insertion of the ethylene,  $\beta$ -hydride transfer/olefin elimination of the product styrene, and the abstraction of proton by  $\text{NEt}_3$  base. The free energy profiles for the pathways involving dipalladium and substrate-bound palladium complexes will be discussed in comparison to monopalladium  $\text{Pd}(\text{PR}_3)$ . In all tables, figures, and schemes, the B3LYP relative enthalpies,

(19) Goossen, L. J.; Koley, D.; Hermann, H. L.; Thiel, W. *Organometallics* **2005**, *24*, 2398–2410.

(20) Goossen, L. J.; Koley, D.; Hermann, H.; Thiel, W. *Chem. Commun.* **2004**, 2141–2143.

(21) Lam, K. C.; Marder, T. B.; Lin, Z. *Organometallics* **2007**, *26*, 758–760.

(22) Surawatanawong, P.; Fan, Y.; Hall, M. B. *J. Organomet. Chem.* **2008**, *693*, 1552–1563.

(23) Ahlquist, M.; Fabrizi, G.; Cacchi, S.; Norrby, P.-O. *J. Am. Chem. Soc.* **2006**, *128*, 12785–12793.

(24) Ahlquist, M. r.; Fabrizi, G.; Cacchi, S.; Norrby, P.-O. *Chem. Commun.* **2005**, 4196–4198.

(25) Frisch, M. J. T.; G. W.; Schlegel, H. B.; Scuseria, G. E.; Robb, M. A.; Cheeseman, J. R.; Montgomery, J. A., Jr.; Vreven, T.; Kudin, K. N.; Burant, J. C.; Millam, J. M.; Iyengar, S. S.; Tomasi, J.; Barone, V.; Mennucci, B.; Cossi, M.; Scalmani, G.; Rega, N.; Petersson, G. A.; Nakatsuji, H.; Hada, M.; Ehara, M.; Toyota, K.; Fukuda, R.; Hasegawa, J.; Ishida, M.; Nakajima, T.; Honda, Y.; Kitao, O.; Nakai, H.; Klene, M.; Li, X.; Knox, J. E.; Hratchian, H. P.; Cross, J. B.; Adamo, C.; Jaramillo, J.; Gomperts, R.; Stratmann, R. E.; Yazyev, O.; Austin, A. J.; Cammi, R.; Pomelli, C.; Ochterski, J. W.; Ayala, P. Y.; Morokuma, K.; Voth, G. A.; Salvador, P.; Dannenberg, J. J.; Zakrzewski, V. G.; Dapprich, S.; Daniels, A. D.; Strain, M. C.; Farkas, O.; Malick, D. K.; Rabuck, A. D.; Raghavachari, K.; Foresman, J. B.; Ortiz, J. V.; Cui, Q.; Baboul, A. G.; Clifford, S.; Cioslowski, J.; Stefanov, B. B.; Liu, G.; Liashenko, A.; Piskorz, P.; Komaromi, I.; Martin, R. L.; Fox, D. J.; Keith, T.; Al-Laham, M. A.; Peng, C. Y.; Nanayakkara, A.; Challacombe, M.; Gill, P. M. W.; Johnson, B.; Chen, W.; Wong, M. W.; Gonzalez, C.; Pople, J. A. *Gaussian03*; Gaussian, Inc.: Pittsburgh, PA, 2003.

(26) Perdew, J. P.; Burke, K.; Ernzerhof, M. *Phys. Rev. Lett.* **1996**, *77*, 3865–3868.

(27) Hay, P. J.; Wadt, W. R. *J. Chem. Phys.* **1985**, *82*, 270–283.

(28) Hay, P. J.; Wadt, W. R. *J. Chem. Phys.* **1985**, *82*, 299–310.

(29) Couty, M.; Hall, M. B. *J. Comput. Chem.* **1996**, *17*, 1359–1370.

(30) Hariharan, P. C.; Pople, J. A. *Theor. Chim. Acta* **1973**, *28*, 213–222.

(31) Petersson, G. A.; Al-Laham, M. A. *J. Chem. Phys.* **1991**, *94*, 6081–6090.

(32) Petersson, G. A.; Bennett, A.; Tensfeldt, T. G.; Al-Laham, M. A.; Shirley, W. A.; Mantzaris, J. J. *J. Chem. Phys.* **1988**, *89*, 2193–2218.

(33) Jong, G. T. d.; Geerke, D. P.; Diefenbach, A.; Bickelhaupt, F. M. *Chem. Phys.* **2005**, *313*, 261–270.

(34) Becke, A. D. *J. Chem. Phys.* **1993**, *98*, 5648. 1993, *98*, 5648.

(35) Lee, C.; Yang, W.; Parr, R. G. *Phys. Rev. B* **1988**, *37*, 785.

(36) Barone, V.; Cossi, M. *J. Phys. Chem. A* **1998**, *102*, 1995.

(37) Cossi, M.; Rega, N.; Scalmani, G.; Barone, V. *J. Comput. Chem.* **2003**, *24*, 669–681.

(38) Wan, S.; Stote, R. H.; Karplus, M. *J. Chem. Phys.* **2004**, *121*, 9539.

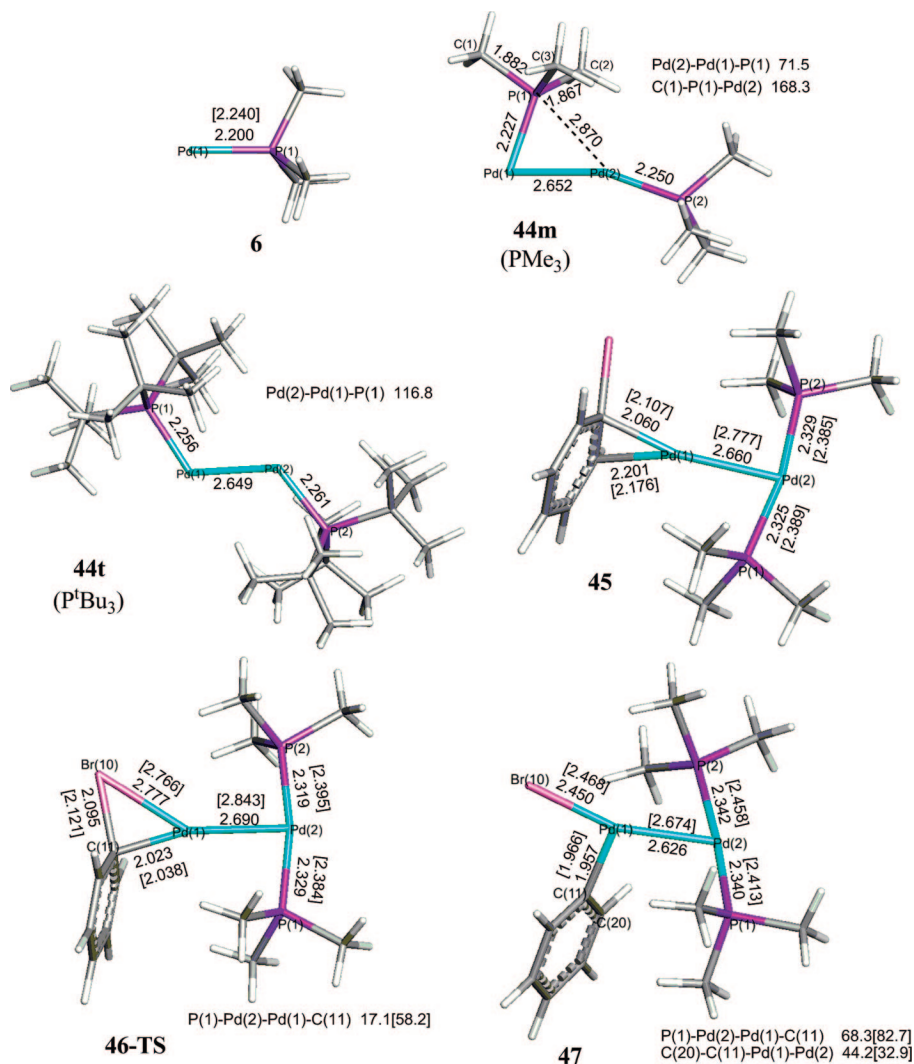


**Figure 1.** Molecular structures in the oxidative addition to dipalladium complex. Calculated bond distances and angles for  $\text{PMe}_3$  and  $\text{P}^t\text{Bu}_3$  (in brackets) are given in Å and deg. Except for **44**, only the structures for  $\text{PMe}_3$  are shown to simplify the figure.

**Table 2.** Relative Enthalpy and Free Energy for the Oxidative Addition to Phosphine-Bound Palladium Complexes ( $\text{R} = \text{Me}, ^t\text{Bu}$ )

|               |  | PMe <sub>3</sub> |                                   |                                 | P <sup>t</sup> Bu <sub>3</sub> |                                   |                                 |
|---------------|--|------------------|-----------------------------------|---------------------------------|--------------------------------|-----------------------------------|---------------------------------|
|               |  | Δ <i>H</i>       | Δ <i>G</i> <sub>gas</sub> (1 atm) | Δ <i>G</i> <sub>tot</sub> (1 M) | Δ <i>H</i>                     | Δ <i>G</i> <sub>gas</sub> (1 atm) | Δ <i>G</i> <sub>tot</sub> (1 M) |
| Dipalladium   |  |                  |                                   |                                 |                                |                                   |                                 |
| <b>1</b>      | Pd <sub>4</sub>  | 0.00             | 0.00                              | 0.00                            | 0.00                           | 0.00                              | 0.00                            |
| <b>6</b>      | Pd(PR <sub>3</sub> )   | 2.26             | 2.02                              | −0.39                           | 2.03                           | 2.20                              | −0.70                           |
| <b>44</b>     | Pd <sub>2</sub> (PR <sub>3</sub> ) <sub>2</sub>                        | −12.43           | −3.53                             | −8.37                           | −12.59                         | −0.50                             | −0.49                           |
| <b>45</b>     | Pd <sub>2</sub> (PR <sub>3</sub> ) <sub>2</sub> (η <sub>2</sub> -PhBr) | −26.43           | −5.78                             | −3.73                           | −21.94                         | 2.98                              | 10.20                           |
| <b>46-TS</b>  | TS1Pd <sub>2</sub> (PR <sub>3</sub> ) <sub>2</sub> (Ph)(Br)            | −23.09           | −1.62                             | 0.43                            | −17.94                         | 7.13                              | 13.54                           |
| <b>47</b>     | Pd <sub>2</sub> (PR <sub>3</sub> ) <sub>2</sub> (Ph)(Br)               | −43.86           | −23.36                            | −24.39                          | −30.86                         | −6.56                             | −1.40                           |
| Monopalladium |  |                  |                                   |                                 |                                |                                   |                                 |
| <b>1</b>      | Pd <sub>4</sub>  | 0.00             | 0.00                              | 0.00                            | 0.00                           | 0.00                              | 0.00                            |
| <b>6</b>      | Pd(PR <sub>3</sub> )   | 2.26             | 2.02                              | −0.39                           | 2.03                           | 2.20                              | −0.70                           |
| <b>18</b>     | Pd(PR <sub>3</sub> )(η <sup>2</sup> -PhBr)                             | −10.36           | −0.96                             | −1.61                           | −12.19                         | −1.46                             | −0.48                           |
| <b>7-TS</b>   | TS1Pd(PR <sub>3</sub> )(Br)(Ph)  | −4.17            | 6.19                              | 5.63                            | −8.75                          | 2.28                              | 2.53                            |
| <b>8</b>      | Pd(PR <sub>3</sub> )(Br)(Ph)   | −25.87           | −16.05                            | −21.31                          | −24.06                         | −13.55                            | −16.67                          |

gas-phase free energies, and free energies with solvent correction are relative to  $\text{Pd}_4 + \text{PR}_3 + \text{PhBr} + \text{C}_2\text{H}_4 + \text{NEt}_3$  except for the ones for dipalladium complexes, which are relative to  $2\text{Pd}_4 + 2\text{PR}_3 + \text{PhBr} + \text{C}_2\text{H}_4 + \text{NEt}_3$ . Unless specified otherwise, the energies mentioned throughout the article refer to the B3LYP relative free energies with solvent correction.

**1. Precatalytic Reaction. (1.1) Ligand/Substrate Binding to Atomic Palladium.** The observation of palladium nanoparticles in the Heck reaction led to suggestions that

the active palladium catalyst is slowly released from the palladium cluster during the reaction cycle.<sup>1-7</sup> The monopalladium leached from the cluster can be stabilized by ligands or substrates (eq 1). Tetranuclear palladium  $\text{Pd}_4$  (**1**) is used as our model for a palladium cluster; the optimized geometry has tetrahedral symmetry with 2.642 Å Pd-Pd bonds. Ligand/substrate binding to a “released” palladium forms a monoligated palladium complex and trinuclear palladium  $\text{Pd}_3$  (**2**), which is trigonal planar with 2.508 Å Pd-Pd bonds. In a comparison to the phosphine ligand, we

**Scheme 1. Solvation (DMSO) Corrected Relative Free Energy (kcal/mol) Profiles for the Oxidative Addition of Phenyl Bromide to Di- and Monopalladium Complexes (in brackets) for  $\text{PMe}_3$  and  $\text{P}^t\text{Bu}_3$  Ligands**

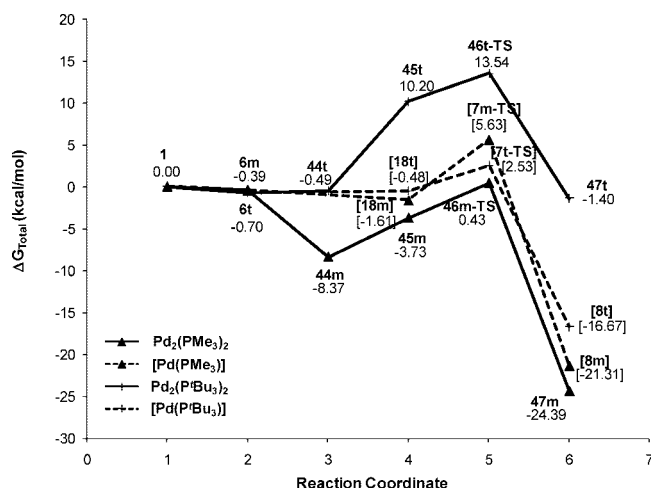
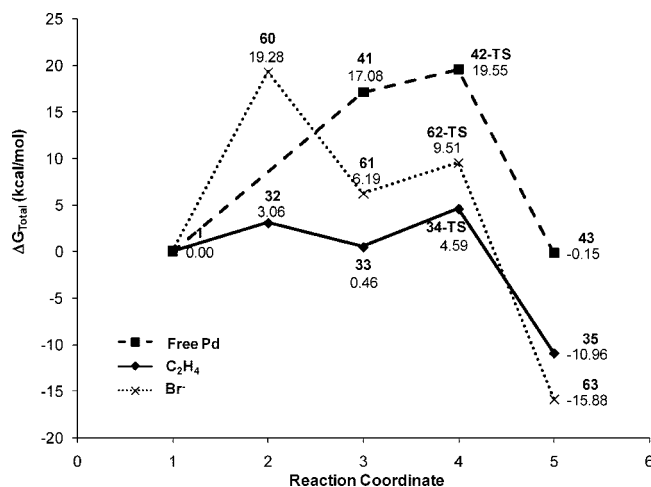


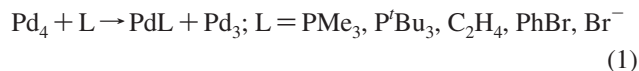
**Table 3. Relative Free Energy for the Oxidative Addition to Substrate-Bound Palladium Complexes**

|  |   | $\Delta H$ | $\Delta G_{\text{gas}}$ (1 atm) | $\Delta G_{\text{tot}}$ (1 M) |
|--|---|------------|---------------------------------|-------------------------------|
| <b><math>\text{C}_2\text{H}_4</math></b> |   |            |                                 |                               |
| 1  | $\text{Pd}_4$   | 0.00       | 0.00                            | 0.00                          |
| 32                                       | $\text{Pd}(\eta^2\text{-C}_2\text{H}_4)$                          | 10.07      | 9.12                            | 3.06                          |
| 33                                       | $\text{InPd}(\eta^2\text{-C}_2\text{H}_4)(\eta^2\text{-PhBr})$    | -2.88      | 6.11                            | 0.46                          |
| 34-TS                                    | $\text{TS1Pd}(\eta^2\text{-C}_2\text{H}_4)(\text{Br})(\text{Ph})$ | 0.75       | 10.56                           | 4.59                          |
| 35                                       | $\text{Pd}(\eta^2\text{-C}_2\text{H}_4)(\text{Br})(\text{Ph})$    | -12.13     | -2.77                           | -10.96                        |
| <b>Free Pd</b>                           |   |            |                                 |                               |
| 1  | $\text{Pd}_4$   | 0.00       | 0.00                            | 0.00                          |
| 41                                       | $\text{Pd}(\eta^2\text{-PhBr})$                                   | 22.41      | 21.50                           | 17.08                         |
| 42-TS                                    | $\text{TS1Pd}(\text{Ph})(\text{Br})$                              | 23.86      | 23.49                           | 19.55                         |
| 43                                       | $\text{Pd}(\text{Ph})(\text{Br})$                                 | 8.75       | 6.09                            | -0.15                         |
| <b><math>\text{Br}^-</math></b>          |   |            |                                 |                               |
| 1  | $\text{Pd}_4$   | 0.00       | 0.00                            | 0.00                          |
| 60                                       | $\text{PdBr}^-$   | 18.39      | 15.14                           | 19.28                         |
| 61                                       | $\text{Pd}(\text{Br})(\eta^2\text{-PhBr})^-$                      | -16.16     | -9.89                           | 6.19                          |
| 62-TS                                    | $\text{TS1Pd}(\text{Br})(\text{Br})(\text{Ph})^-$                 | -12.48     | -6.60                           | 9.51                          |
| 63                                       | $\text{Pd}(\text{Br})(\text{Br})(\text{Ph})^-$                    | -41.35     | -35.78                          | -15.88                        |

**Scheme 2. Solvation (DMSO) Corrected Relative Free Energy (kcal/mol) Profiles for the Oxidative Addition of Phenyl Bromide to Substrate-Bound and Free Palladium ( $\text{Pd}(\eta^2\text{-C}_2\text{H}_4)$ ,  $\text{PdBr}^-$ , and  $\text{Pd}$ )**



examined the stability of palladium binding with substrates, which are ethylene, phenyl bromide, and bromide ion, to mimic the “ligand-free” condition.



When phosphine binds to palladium, the formation of palladium monophosphine,  $\text{PdPR}_3$ , and trinuclear palladium from the tetranuclear palladium and phosphine is exergonic by  $-0.39$  and  $-0.70$  kcal/mol for  $\text{PdPMe}_3$  (**6m**) and  $\text{PdP}^t\text{Bu}_3$  (**6t**), respectively (Table 1). The similar reaction for substrate binding leads to the formation of  $\text{Pd}(\eta^2\text{-C}_2\text{H}_4)$  (**32**) and  $\text{Pd}(\eta^2\text{-PhBr})$  (**41**) complexes with the energy changes of 3.06 and 17.08 kcal/mol, respectively. The  $\pi$ -donor and  $\pi^*$ -acceptor in the ethylene play the same role in stabilizing Pd as the lone-pair donor and  $\sigma^*$ -acceptor in the phosphine. The PhBr binds more weakly to palladium in part because the binding decreases the conjugation of the aromatic ring. De Vries proposed that halide ions play a role to stabilize atomic palladium in the “ligand-free” mechanism for the Heck reaction.<sup>2,4</sup> In our calculation, the formation of  $\text{PdBr}^-$  produces an energy change of 19.28 kcal/mol. The high free energy change corresponds to the fact that bromide ion has  $\pi$ -donor but no  $\pi$ -acceptor capacity; therefore, without the back-bonding interaction, the bromide ion is a poorer ligand than ethylene for the electron-rich Pd atom.

These initial results show that the atomic palladium leached from a palladium cluster is stabilized by phosphine ligands in the presence of phosphines, but, in the absence of phosphine, the ethylene serves as a better ligand than either phenyl bromide or bromide ion.

**(1.2) Dipalladium Formation.** Experimentally, dipalladium complexes were found with the bridging ligands,<sup>39</sup> e.g., diene,<sup>40</sup> allene,<sup>41</sup> halogen,<sup>42,43</sup> and phosphine.<sup>44</sup> We examined the dimerization of palladium monophosphine to form the dipalladium diphosphine  $\text{Pd}_2(\text{PR}_3)_2$  **44** ( $\text{R} = \text{Me}$  and  $^t\text{Bu}$  for **44m** and **44t**, respectively). With the  $\text{PMe}_3$  ligand, the  $\text{Pd}(1)\text{--Pd}(2)$  bond distance in **44m** is 2.652 Å (Figure 1) and one phosphine ligand is semibridging between the two palladiums with a strong  $\text{Pd}(1)\text{--P}(1)$  bond, 2.227 Å, and a weak  $\text{Pd}(2)\text{--P}(1)$  bond, 2.870 Å. The other phosphine is attached solely to one palladium; the  $\text{Pd}(2)\text{--P}(2)$  bond is 2.250 Å. In the semibridging interaction, the  $\text{Pd}(1)\text{--P}(1)$  bond tilts toward the neighboring  $\text{Pd}(2)$  atom to form a three-center four-electron bond ( $\text{C}(1)\text{--P}(1)\text{--Pd}(2)$  bond);  $\text{P}(1)$  begins to take on a five-coordinate hypervalent (expanded octet) structure. The  $\text{P}^t\text{Bu}_3$  ligand's steric bulk prevents the bridging geometry; structure **44t** is nearly symmetrical. With the semibridging coordination of phosphine, the dipalladium structure **44m** is stabilized to  $-8.37$  kcal/mol, whereas without the semibridging phosphine, structure **44t** is stabilized only to  $-0.49$  kcal/mol (Table 2 and Scheme 1).

**2. Oxidative Addition to Dipalladium,  $\text{Pd}_2(\text{PR}_3)_2$ .** In the formation of the  $\pi$ -bound complex  $\text{Pd}_2(\text{PR}_3)_2(\eta^2\text{-PhBr})$  **45**, both phosphines migrate to one palladium while the other palladium forms  $\pi$ -interaction with the phenyl bromide. The energies are  $-3.73$  and  $10.20$  kcal/mol for  $\text{PMe}_3$  (**45m**) and  $\text{P}^t\text{Bu}_3$  (**45t**), respectively (Table 2 and Scheme 1). The much higher energy for  $\text{P}^t\text{Bu}_3$  in comparison to  $\text{PMe}_3$  arises from

(39) Jain, V. K.; Jain, L. *Coord. Chem. Rev.* **2005**, 249, 3075–3197.

(40) Murahashi, T.; Kanehisa, N.; Kai, Y.; Otani, T.; Kurosawa, H. *Chem. Commun.* **1996**, 825.

(41) Ogoshi, S.; Tsutsumi, K.; Ooi, M.; Kurosawa, H. *J. Am. Chem. Soc.* **1995**, 117, 10415–10416.

(42) Dura-Vila, V.; Mingos, D. M. P.; Vilar, R.; White, A. J. P.; Williams, D. J. *J. Organomet. Chem.* **2000**, 600, 198–205.

(43) Vilar, R.; Mingos, D. M. P.; Cardin, C. J. *J. Chem. Soc., Dalton Trans.* **1996**, 4313–4314.

(44) Budzelaar, P. H. M.; van Leeuwen, P. W. V. M.; Robeeck, C. F.; Orpen, A. G. *Organometallics* **1992**, 11, 23–25.

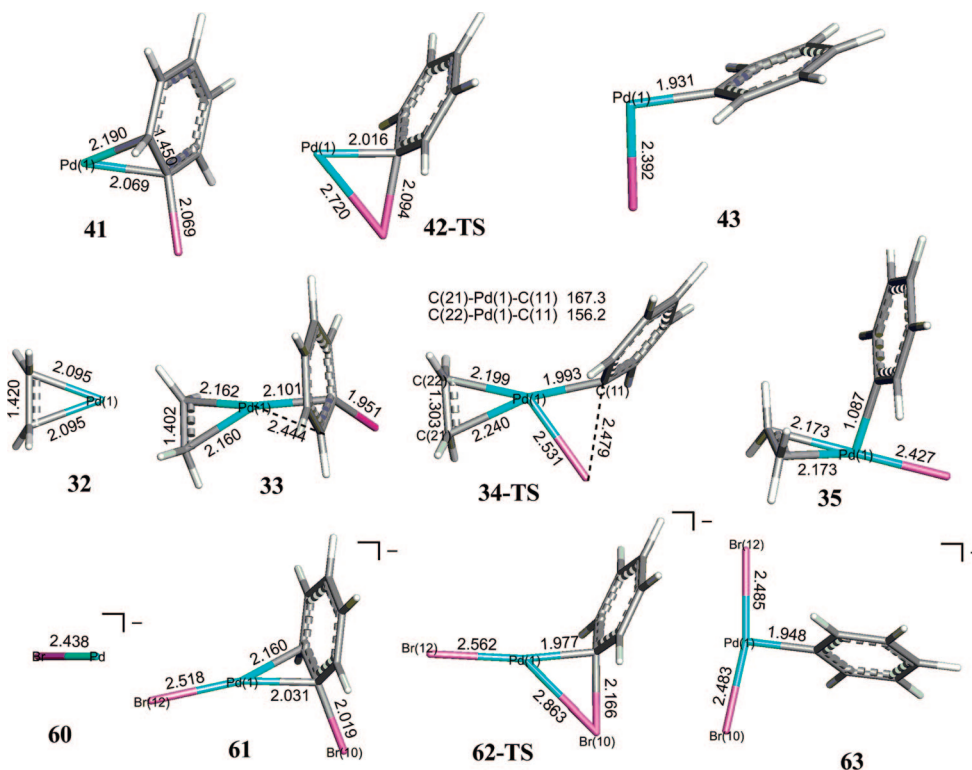
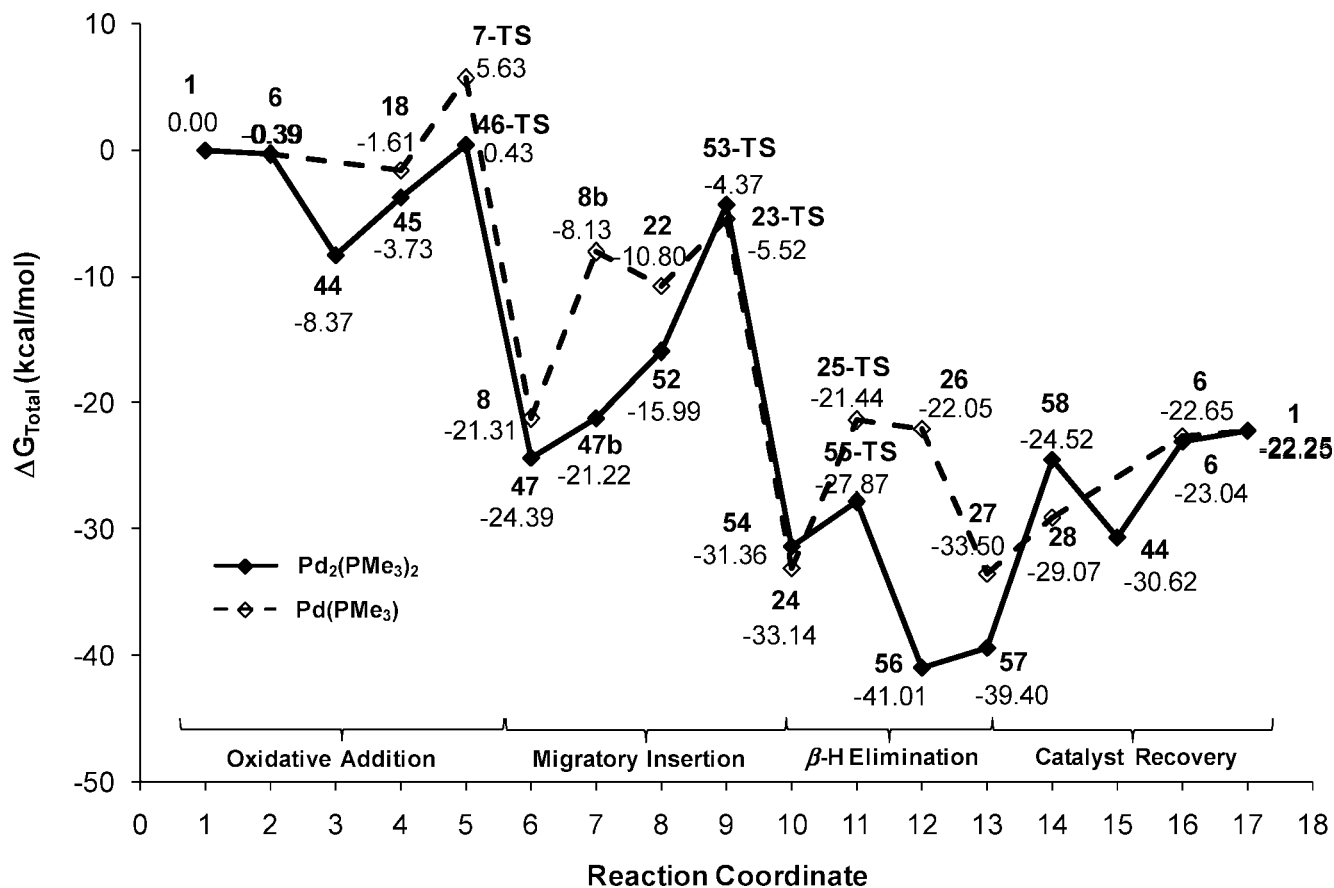


**Figure 2.** Molecular structures in the oxidative addition to substrate-bound palladium complex. Calculated bond distances and angles are given in Å and deg.

**Scheme 3.** Solvation (DMSO) Corrected Relative Free Energy (kcal/mol) Profiles of the Heck Catalytic Cycle in the Oxidative Addition, Migratory Insertion,  $\beta$ -H Transfer/Olefin Elimination, and Catalyst Recovery by Mono- and Dipalladium Complexes with the  $\text{PMe}_3$  Ligand



the steric interaction, leading to weaker Pd–Pd and Pd–P bonds; the Pd–Pd and Pd–P bond distances are 0.12 and

0.06 Å longer in **45t** than in **45m**. Then, the oxidative addition proceeds through transition state **46-TS**. In **46-TS**, the phenyl

**Table 4. Relative Enthalpy and Free Energy for the Migratory Insertion,  $\beta$ -Hydride/Olefin Transfer Elimination, and Catalyst Recovery for Di- and Monopalladium Complexes**

|  |              |   | $\Delta H$ | $\Delta G_{\text{gas}}$ (1 atm) | $\Delta G_{\text{tot}}$ (1 M) |
|--|--------------|---|------------|---------------------------------|-------------------------------|
| Dipalladium                            |              |   |            |                                 |                               |
| migratory insertion                    | <b>47</b>    | $\text{Pd}_2(\text{PMe}_3)_2(\text{Ph})(\text{Br})$                               | -43.86     | -23.36                          | -24.39                        |
|  | <b>47b</b>   | $\text{Pd}_2(\text{PMe}_3)_2(\text{Ph})(\text{Br})\text{b}$                       | -39.61     | -19.90                          | -21.22                        |
|  | <b>52</b>    | $\text{Pd}_2(\text{PMe}_3)_2(\text{Ph})(\text{Br})(\text{C}_2\text{H}_4)$         | -48.13     | -16.42                          | -15.99                        |
|  | <b>53-TS</b> | $\text{TS2Pd}_2(\text{PMe}_3)_2(\text{Ph})(\text{Br})(\text{C}_2\text{H}_4)$      | -37.28     | -3.33                           | -4.37                         |
| $\beta$ -H transfer/olefin elimination | <b>54</b>    | $\text{Pd}_2(\text{PMe}_3)_2(\text{Br})(\text{HC}_2\text{H}_3\text{Ph})$          | -61.51     | -28.88                          | -31.36                        |
|  | <b>55-TS</b> | $\text{TS3Pd}_2(\text{PMe}_3)_2(\text{Br})(\text{HC}_2\text{H}_3\text{Ph})$       | -57.55     | -25.02                          | -27.87                        |
|  | <b>56</b>    | $\text{Pd}_2(\text{PMe}_3)_2(\text{Br})(\text{H})(\text{C}_2\text{H}_3\text{Ph})$ | -68.19     | -38.10                          | -41.01                        |
| catalyst recovery                      | <b>57</b>    | $\text{Pd}_2(\text{PMe}_3)_2(\text{Br})(\text{H})$                                | -50.92     | -31.51                          | -39.40                        |
|  | <b>58</b>    | $\text{Pd}_2(\text{PMe}_3)_2(\text{Br})(\text{H}-\text{NEt}_3)$                   | -53.43     | -21.62                          | -24.52                        |
|  | <b>44</b>    | $\text{Pd}_2(\text{PMe}_3)_2$   | 67.81      | 81.30                           | -30.62                        |
|  | <b>6</b>     | $\text{Pd}(\text{PMe}_3)$   | 84.75      | 88.86                           | -23.04                        |
|  | <b>1</b>     | $\text{Pd}_4$   | 80.23      | 84.83                           | -22.25                        |
| Monopalladium                          |              |   |            |                                 |                               |
| migratory insertion                    | <b>8</b>     | $\text{Pd}(\text{PMe}_3)(\text{Br})(\text{Ph})$                                   | -25.87     | -16.05                          | -21.31                        |
|  | <b>8b</b>    | $\text{Pd}(\text{PMe}_3)(\text{Br})(\text{Ph})\text{b}$                           | -14.51     | -5.86                           | -8.13                         |
|  | <b>22</b>    | $\text{Pd}(\text{PMe}_3)(\text{Br})(\text{Ph})(\eta^2\text{-C}_2\text{H}_4)$      | -25.04     | -3.76                           | -10.80                        |
|  | <b>23-TS</b> | $\text{TS2Pd}(\text{PMe}_3)(\text{Br})(\text{Ph})(\text{C}_2\text{H}_4)$          | -20.13     | 1.97                            | -5.52                         |
| $\beta$ -H transfer/olefin elimination | <b>24</b>    | $\text{Pd}(\text{PMe}_3)(\text{Br})(\text{HC}_2\text{H}_3\text{Ph})$              | -47.84     | -25.87                          | -33.14                        |
|  | <b>25-TS</b> | $\text{TS3Pd}(\text{PMe}_3)(\text{Br})(\text{HC}_2\text{H}_3\text{Ph})$           | -36.97     | -14.26                          | -21.44                        |
|  | <b>26</b>    | $\text{Pd}(\text{PMe}_3)(\text{Br})(\text{H})(\text{C}_2\text{H}_3\text{Ph})$     | -36.58     | -15.45                          | -22.05                        |
| catalyst recovery                      | <b>27</b>    | $\text{Pd}(\text{PMe}_3)(\text{Br})(\text{H})$                                    | -34.53     | -25.88                          | -33.50                        |
|  | <b>28</b>    | $\text{Pd}(\text{PMe}_3)(\text{Br})(\text{H}-\text{NEt}_3)$                       | -43.21     | -20.40                          | -29.07                        |
|  | <b>6</b>     | $\text{Pd}(\text{PMe}_3)$   | 82.49      | 86.84                           | -22.65                        |
|  | <b>1</b>     | $\text{Pd}_4$   | 80.23      | 84.83                           | -22.25                        |

ring twists about the Pd(1)–C(11) bond to avoid steric interactions with the phosphines; the dihedral angles P(1)–Pd(2)–Pd(1)–C(11) are 17.1° and 58.2° for **46m-TS** and **46t-TS**, respectively. The energy barriers relative to the  $\pi$ -complex **45m** and **45t** are similar for **46m-TS** and **46t-TS**, 4.16 and 3.34 kcal/mol, respectively. Therefore, the main contributions to the difference in overall reaction barrier at **46-TS** for different phosphines are from (i) the dimerization of monopalladium monophosphine and (ii) the rearrangement of the phosphine ligands to be on the same palladium center to open the other palladium for coordination with phenyl bromide. Finally, the reaction coordinate leads from **46-TS** to the stable intermediate  $\text{Pd}_2(\text{PR}_3)_2(\text{Ph})(\text{Br})$  **47** with energies of -24.39 and -1.40 kcal/mol for **47m** and **47t**, respectively. The phenyl ring is twisted further in these intermediates as the P(1)–Pd(2)–Pd(1)–C(11) dihedral angles have increased to 68.3° and 82.7°, respectively.

In our previous study of monopalladium with various ligands, the palladium monophosphine provided the lowest pathway to phenyl bromide oxidative addition.<sup>22</sup> The energies for the mono- and dipalladium complex are compared in Table 2 and Scheme 1. For monopalladium monophosphine, the better  $\sigma$ -donor ligand ( $\text{P}^t\text{Bu}_3$  vs  $\text{PMe}_3$ ) produces a lower barrier for the oxidative-addition transition state (**7-TS**) relative to the phenyl bromide  $\pi$ -complex (**18**), 7.24 and 3.01 kcal/mol for **7m-TS** and **7t-TS**, respectively. For dipalladium diphosphine, in contrast, the energy barriers of the transition state (**46-TS**) relative to the  $\pi$ -complex (**45**) are similar for **46m-TS** and **46t-TS**, 4.16 and 3.34 kcal/mol, respectively. In the dipalladium complex, the neighboring  $\text{Pd}(\text{PMe}_3)_2$  served as a ligand to the active palladium and as a better  $\sigma$ -donor than  $\text{PMe}_3$  alone, producing a lower barrier. The steric effect of the phosphine substituents is also important for the energy of the transition state. The steric hindrance of  $\text{P}^t\text{Bu}_3$  causes more difficulty in the formation of dipalladium diphosphine and its  $\pi$ -complex, the main contribution to the

free energy of the oxidative-addition transition state (**46-TS**). For the small phosphine ligand,  $\text{PMe}_3$ , the monopalladium transition state (**7m-TS**) is 5.20 kcal/mol higher than the dipalladium transition state (**46m-TS**), whereas for large phosphine ligand,  $\text{P}^t\text{Bu}_3$ , **7t-TS** is -11.01 kcal/mol lower than **46t-TS**. Thus, for small phosphine ligands, such as  $\text{PMe}_3$ , phenyl bromide oxidative addition can proceed not only on monopalladium monophosphine but also on dipalladium diphosphine complexes. On the other hand, for the sterically hindered phosphine ligands, such as  $\text{P}^t\text{Bu}_3$ , phenyl bromide oxidative addition on monopalladium monophosphine is preferred to that on dipalladium diphosphine.

**3. Oxidative Addition to Substrate-Bound Palladium.** In the absence of phosphine ligands, both free Pd atoms and Pd bound to other substrate molecules, acting as supporting ligands, can initiate the oxidative addition of PhBr. The energies for the oxidative addition of PhBr on free Pd,  $\text{Pd}(\eta^2\text{-C}_2\text{H}_4)$ , and  $\text{PdBr}^-$  are presented in Table 3 and Scheme 2, and the related structures are shown in Figure 2. The formation of  $\text{Pd}(\eta^2\text{-PhBr})$  **41** from the  $\text{Pd}_4$  cluster causes an energy increase of 17.08 kcal/mol. Then, **41** completes the oxidative addition via **42-TS** (19.55 kcal/mol), forming  $\text{Pd}(\text{Ph})(\text{Br})$  **43** at -0.15 kcal/mol. The main contribution for the oxidative addition barrier on atomic Pd is derived mainly from the formation of  $\pi$ -bound phenyl bromide palladium complex from  $\text{Pd}_4$ .

Formation of  $\text{Pd}(\eta^2\text{-C}_2\text{H}_4)$  **32** from  $\text{Pd}_4$  is more facile (3.06 kcal/mol) because of the strong  $\pi$ -acceptor properties of  $\text{C}_2\text{H}_4$ . The C–C bond length increases by 0.08 Å on formation of  $\text{Pd}(\eta^2\text{-C}_2\text{H}_4)$ . The palladium in **32** forms  $\pi$ -bound phenyl bromide complex  $\text{Pd}(\eta^2\text{-C}_2\text{H}_4)(\eta^2\text{-PhBr})$  **33** (0.46 kcal/mol); then, oxidative addition via transition state **34-TS** proceeds with a low barrier (4.59 kcal/mol). In the transition state structure, the two Pd–C bonds to ethylene are not equivalent; since C(21) is nearly colinear with the phenyl group, which has a high trans-influence group, Pd–C(21) is longer than Pd–C(22) by 0.04 Å (Figure 2). With the formation of the T-shaped intermediate  $\text{Pd}(\eta^2\text{-C}_2\text{H}_4)(\text{Br})(\text{Ph})$

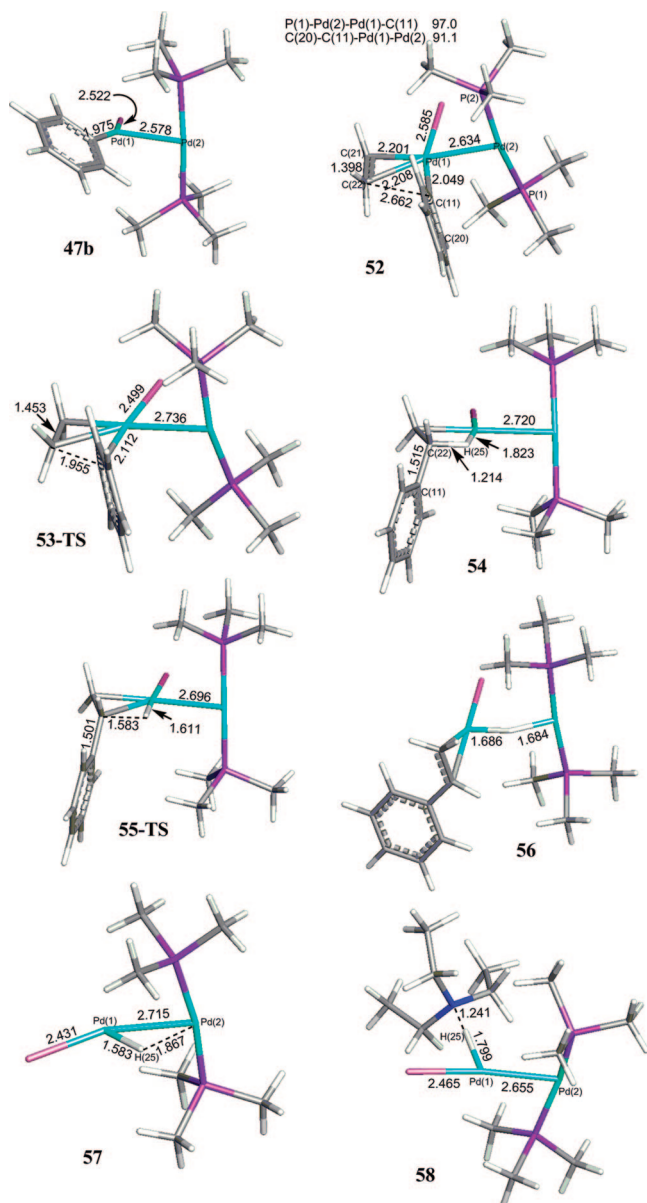


**Figure 3.** Molecular structures in the migratory insertion,  $\beta$ -transfer/olefin elimination, and catalyst recovery of dipalladium complex with  $\text{PMe}_3$  ligand. Calculated bond distances and angles are given in Å and deg.

**35**, the phenyl group is now trans to the empty site and the energy decreases to  $-10.96$  kcal/mol.

Formation of  $[\text{PdBr}]^-$  **60** causes an energy increase of 19.28 kcal/mol. Then, the phenyl bromide binds to **60**, forming  $[\text{Pd}(\text{Br})(\eta^2\text{-PhBr})]^-$  **61** (6.19 kcal/mol), before proceeding to the oxidative-addition transition state **62-TS** with an energy of 9.51 kcal/mol (Table 3 and Scheme 2). Following **62-TS**, the system rearranges to the intermediate  $[\text{Pd}(\text{Br})(\text{Br})(\text{Ph})]^-$  **63**, in which two bromides are trans to each other and the phenyl group is trans to the empty site; the energy decreases to  $-15.88$  kcal/mol. Interestingly, the rate-limiting step here is the formation of  $\text{PdBr}^-$ .

Of all of the phosphine-free palladium complexes,  $\text{Pd}(\eta^2\text{-C}_2\text{H}_4)$  **32** is clearly preferred for phenyl bromide oxidative addition. The  $\pi$ -donor and  $\pi^*$ -acceptor character of ethylene allows it to play a similar role to the phosphine in stabilizing atomic palladium. Although its transition state energy (**34-TS**) is comparable to **7m-TS**, it is still higher than **46m-TS** and **7t-**

**TS**. Therefore, in the presence of phosphine ligands, the oxidative addition still prefers to proceed via palladium stabilized by phosphine ligand(s). However, in the absence of phosphine, the oxidative addition of phenyl bromide can proceed quite easily via ethylene-supported palladium,  $\text{Pd}(\eta^2\text{-C}_2\text{H}_4)$  **32**.

**4. Migratory Insertion,  $\beta$ -Hydride Elimination, and Catalyst Recovery of Dipalladium Complexes.** Because the oxidative-addition step through the dipalladium diphosphine complex is unlikely for the sterically hindered  $\text{P}^t\text{Bu}_3$  ligand, we calculated the rest of the Heck reaction for the dipalladium diphosphine only for the  $\text{PMe}_3$  ligand. The energy barrier for the phenyl bromide oxidative addition via dipalladium is lower than the monopalladium complex by  $-5.20$  kcal/mol for the  $\text{PMe}_3$  ligand. The energies for the entire Heck reaction path through the  $\text{Pd}_2(\text{PMe}_3)_2$  catalyst are shown and compared with the reaction path through  $\text{Pd}(\text{PMe}_3)$  in Scheme 3 and Table 4.

Phenyl bromide oxidative addition produces  $\text{Pd}_2(\text{PMe}_3)_2(\text{Ph})(\text{Br})$  **47**, in which the phenyl ring twists about the  $\text{Pd}(1)\text{--C}(11)$  bond to reduce the steric interaction with the phosphines (Figure 1). Intermediate **47**, then, rearranges to **47b** with the neighboring palladium trans to the empty site; the  $\text{Pd}(1)\text{--Pd}(2)$  bond shortens from 2.626 Å to 2.578 Å and the  $\text{Pd}(1)\text{--Br}(10)$  bond lengthens from 2.450 Å to 2.522 Å (Figures 1 and 3). The phenyl, the highest trans-influence ligand, trans to the empty site in **47**, is now trans to the bromide ion in **47b**; therefore, the isomerization causes an energy increase from  $-24.39$  to  $-21.22$  kcal/mol (Table 4).

Ethylene now binds at the empty site cis to the phenyl group to form  $\text{Pd}_2(\text{PMe}_3)_2(\text{Ph})(\text{Br})(\text{C}_2\text{H}_4)$  **52**. The active Pd is in a nearly square-planar environment with both ethylene carbons lying parallel to the coordination plane and perpendicular to the  $\text{P}(1)\text{--Pd}(2)\text{--P}(2)$  plane. The ethylene binding causes an energy increase to  $-15.99$  kcal/mol. Then, **52** proceeds to the migratory insertion via **53-TS**. The phenyl group in **53-TS** bends back toward phosphine substituents on the neighbor palladium. To reduce steric interaction, the  $\text{Pd}(1)\text{--Pd}(2)$  bond is lengthened further by 0.10 Å; the energy increases to  $-4.37$  kcal/mol. In completing this step, the phenyl group migrates to the nearest ethylene C(22) and then moves away from the Pd, which leaves a C–H agostic bond interaction to palladium where the phenyl was previously attached.

From the intermediate formed,  $\text{Pd}_2(\text{PMe}_3)_2(\text{Br})(\text{HCH}_2\text{CHPh})$  **54** ( $-31.36$  kcal/mol), the agostic  $\beta$ -hydrogen H(25) transfers from C(22) to palladium via **55-TS**, increasing in energy to  $-27.87$  kcal/mol. Relative to **54**, the  $\text{Pd}(1)\text{--H}(25)$  bond is shortened by 0.21 Å and the  $\text{C}(22)\text{--H}(25)$  bond is lengthened by 0.37 Å in **55-TS**. The intermediate product **56** is formed at  $-41.01$  kcal/mol, the hydrogen H(25) atom is found bridging equally between the two palladium ( $\text{Pd--H} \approx 1.68$  Å), and the  $\text{Pd}(1)\text{--Pd}(2)$  bond lengthens to 3.17 Å. In **56**, the styrene group is bound trans to bromide and the  $\text{C}(21)\text{--C}(22)$  bond is perpendicular to the coordination plane. Then, the dissociation of the styrene product is slightly endergonic relative to **56** (1.61 kcal/mol) and leads to  $\text{Pd}_2(\text{PMe}_3)_2(\text{Br})(\text{H})$  **57**. The hydrogen atom becomes semibridging between two palladium atoms; the  $\text{Pd}(1)\text{--H}(25)$  and  $\text{Pd}(2)\text{--H}(25)$  bond distances are 1.583 and 1.867 Å, respectively, and the  $\text{Pd}(1)\text{--Pd}(2)$  bond shortens to 2.715 Å.

To recover the active catalyst, the base  $\text{NEt}_3$  abstracts the proton and forms  $\text{Pd}_2(\text{PMe}_3)_2(\text{Br})(\text{H--NEt}_3)$  **58** ( $-24.52$  kcal/mol). Now, the hydrogen H(25) is bound in between N and Pd(1) and the  $\text{Pd}(1)\text{--Pd}(2)$  bond shortens further to 2.655 Å.

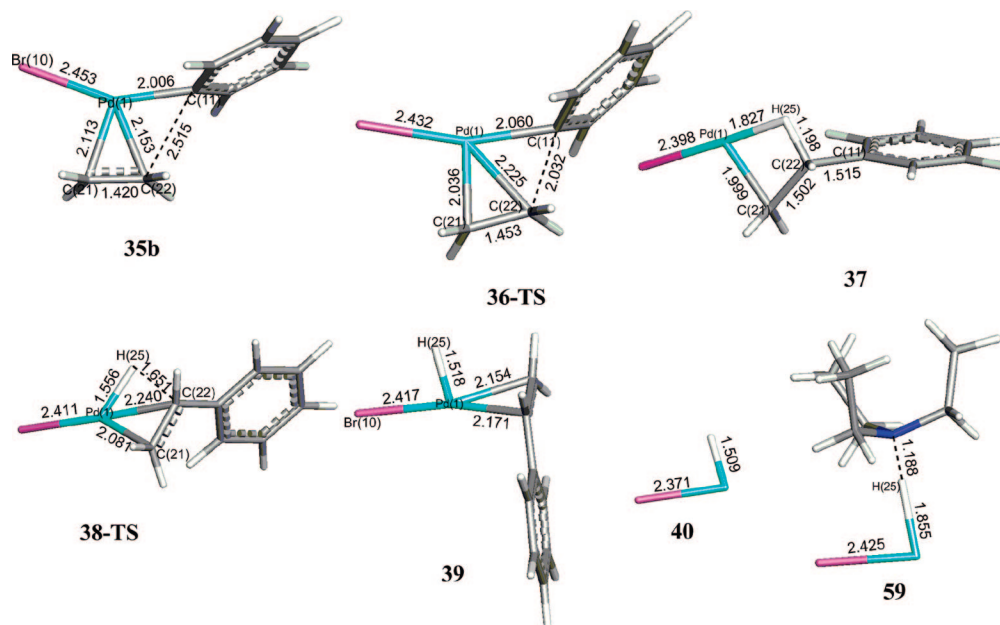


**Figure 4.** Molecular structures in the migratory insertion,  $\beta$ -H transfer/olefin elimination, and catalyst recovery of ethylene-bound palladium complex. Calculated bond distances and angles are given in Å and deg.

Elimination of  $\text{HNEt}_3^+$  and  $\text{Br}^-$  and the formation of  $\text{Pd}_2(\text{PMe}_3)_2$  **44** reduces the energy to  $-30.62$  kcal/mol. This active catalyst can start the catalytic reaction again or the complete cycle leads back to  $\text{Pd}_4$  and phosphine losses with an energy of  $-22.25$  kcal/mol.

The free energy profiles of the Heck reaction through  $\text{Pd}(\text{PMe}_3)$  and  $\text{Pd}_2(\text{PMe}_3)_2$  are compared in Scheme 3; the structures of all species related to the pathway of  $\text{Pd}(\text{PMe}_3)^{22}$  are shown in the Supporting Information. Since the energies of the species along the reaction coordinate involving

**Scheme 4.** Solvation (DMSO) Corrected Relative Free Energy (kcal/mol) Profiles of the Heck Catalytic Cycle in the Oxidative Addition, Migratory Insertion,  $\beta$ -H Transfer/Olefin Elimination, and Catalyst Recovery by Substrate-Bound Palladium Complexes

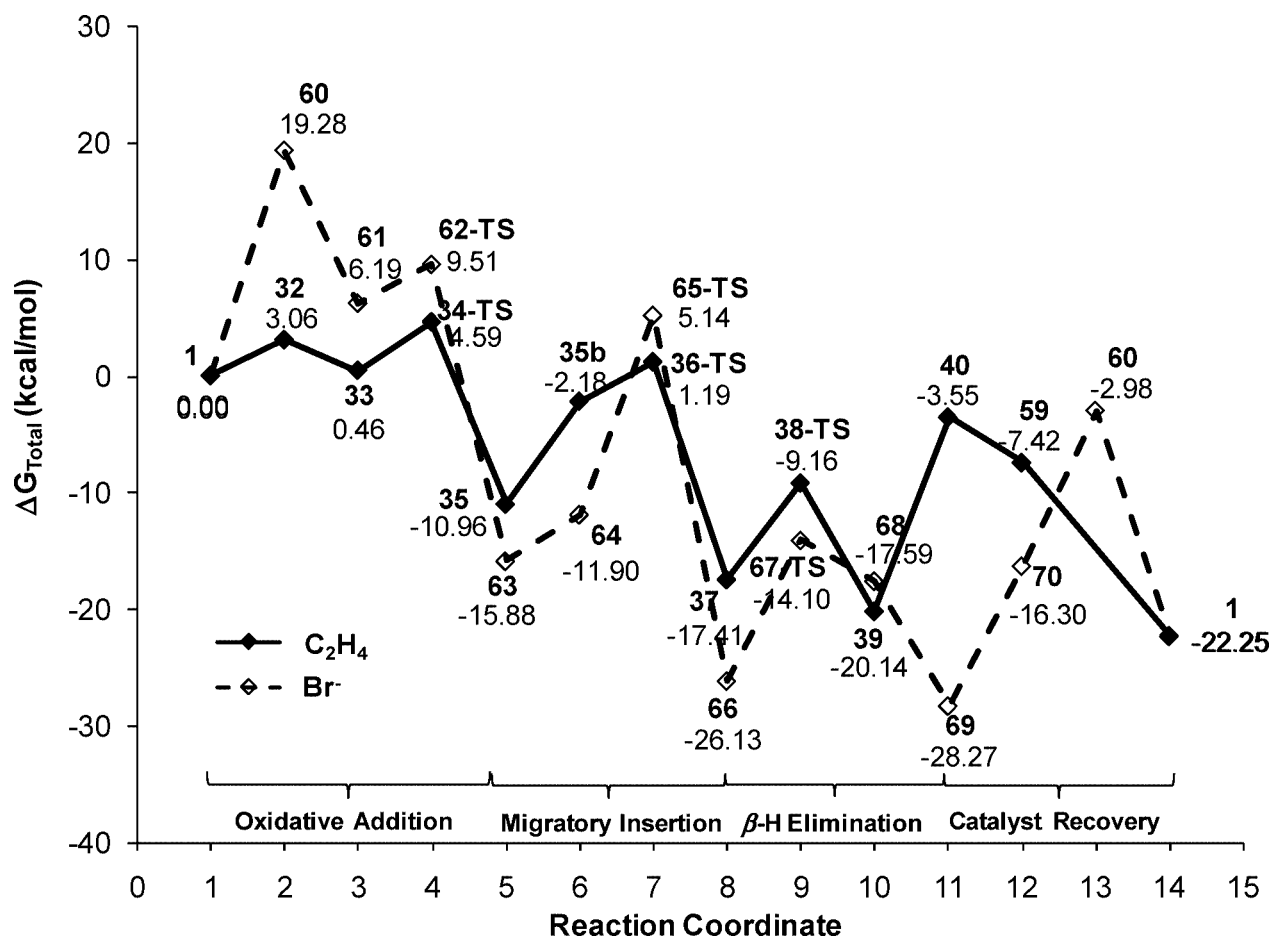


**Table 5.** Relative Enthalpy and Free Energy for the Migratory Insertion,  $\beta$ -Hydride/Olefin Transfer Elimination, and Catalyst Recovery for Substrate-Bound Palladium Complexes

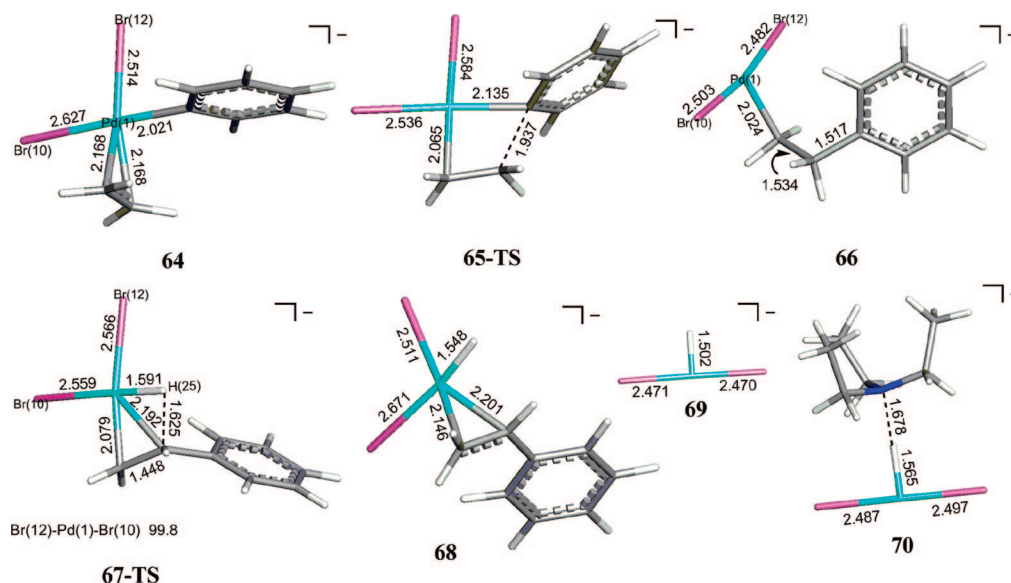
|  |              |  | $\Delta H$ | $\Delta G_{\text{gas}}$ (1 atm) | $\Delta G_{\text{tot}}$ (1 M) |
|--|--------------|--|------------|---------------------------------|-------------------------------|
| $\text{C}_2\text{H}_4$                 |              |  |            |                                 |                               |
| migratory insertion                    | <b>35</b>    | $\text{Pd}(\eta^2\text{-C}_2\text{H}_4)(\text{Br})(\text{Ph})$               | -12.13     | -2.77                           | -10.96                        |
|  | <b>35b</b>   | $\text{Pd}(\eta^2\text{-C}_2\text{H}_4)(\text{Br})(\text{Ph})\text{b}$       | -1.97      | 6.25                            | -2.18                         |
|  | <b>36-TS</b> | $\text{TS2Pd}(\eta^2\text{-C}_2\text{H}_4)(\text{Br})(\text{Ph})$            | 0.67       | 11.22                           | 1.19                          |
| $\beta$ -H transfer/olefin elimination | <b>37</b>    | $\text{Pd}(\text{Br})(\text{HC}_2\text{H}_3\text{Ph})$                       | -17.50     | -7.58                           | -17.41                        |
|  | <b>38-TS</b> | $\text{TS3Pd}(\text{Br})(\text{HC}_2\text{H}_3\text{Ph})$                    | -9.24      | 0.17                            | -9.16                         |
|  | <b>39</b>    | $\text{Pd}(\text{Br})(\text{H})(\text{C}_2\text{H}_3\text{Ph})$              | -21.27     | -11.85                          | -20.14                        |
| catalyst recovery                      | <b>40</b>    | $\text{Pd}(\text{Br})(\text{H})$   | 7.36       | 5.08                            | -3.55                         |
|  | <b>59</b>    | $\text{Pd}(\text{Br})(\text{H-NEt}_3)$                                       | -6.08      | 4.79                            | -7.42                         |
|  | <b>1</b>     | $\text{Pd}_4$  | 80.23      | 84.83                           | -22.25                        |
| $\text{Br}^-$                          |              |  |            |                                 |                               |
| migratory insertion                    | <b>63</b>    | $\text{Pd}(\text{Br})(\text{Br})(\text{Ph})^-$                               | -41.35     | -35.78                          | -15.88                        |
|  | <b>64</b>    | $\text{Pd}(\text{Br})(\text{Br})(\text{Ph})(\text{C}_2\text{H}_4)^-$         | -44.35     | -27.03                          | -11.90                        |
|  | <b>65-TS</b> | $\text{TS2Pd}(\text{Br})(\text{Br})(\text{Ph})(\text{C}_2\text{H}_4)^-$      | -22.92     | -5.07                           | 5.14                          |
| $\beta$ -H transfer/olefin elimination | <b>66</b>    | $\text{InPd}(\text{Br})(\text{Br})(\text{HC}_2\text{H}_3\text{Ph})^-$        | -61.43     | -44.30                          | -26.13                        |
|  | <b>67-TS</b> | $\text{TS3Pd}(\text{Br})(\text{Br})(\text{HC}_2\text{H}_3\text{Ph})^-$       | -43.48     | -25.73                          | -14.10                        |
|  | <b>68</b>    | $\text{Pd}(\text{Br})(\text{Br})(\text{H})(\text{C}_2\text{H}_3\text{Ph})^-$ | -49.13     | -31.42                          | -17.59                        |
| catalyst recovery                      | <b>69</b>    | $\text{Pd}(\text{Br})(\text{Br})(\text{H})^-$                                | -48.19     | -43.18                          | -28.27                        |
|  | <b>70</b>    | $\text{Pd}(\text{Br})(\text{Br})(\text{H-NEt}_3)^-$                          | -47.66     | -30.79                          | -16.30                        |
|  | <b>60</b>    | $\text{PdBr}^-$  | 98.63      | 99.96                           | -2.98                         |
|  | <b>1</b>     | $\text{Pd}_4$  | 80.23      | 84.83                           | -22.25                        |

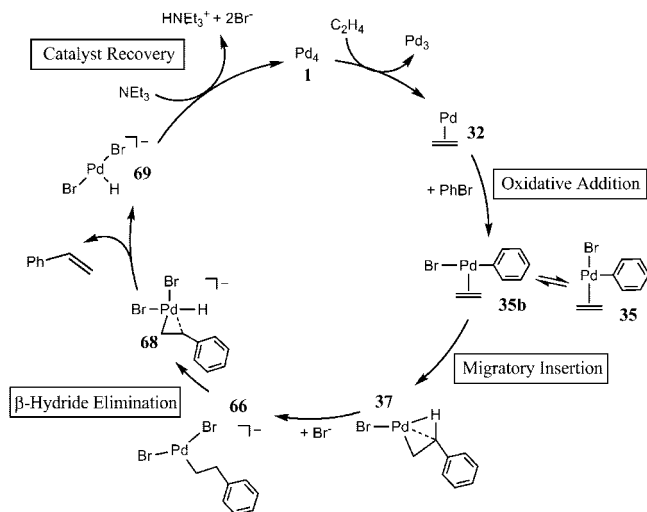
$\text{Pd}_2(\text{PMe}_3)_2$  are similar to or lower than those involving  $\text{PdPMe}_3$ , dipalladium complexes could easily be involved in the Heck catalytic cycle with small phosphines or even other small supporting ligands.

**5. Migratory Insertion,  $\beta$ -Hydride Elimination, and Catalyst Recovery of Substrated-Bound Palladium Complexes. (5.1) Ethylene-Bound Palladium Complex.** In the absence of phosphine, ethylene-bound Pd can provide a low-energy oxidative-addition barrier. The intermediate **35** rearranges to place the ethylene parallel to the coordination plane and the phenyl group trans to the bromide ion (Figures 2 and 4); the energy increases from -10.96 (**35**) to -2.18 kcal/mol (**35b**) (Scheme 4 and Table 5). Then, the migratory insertion proceeds through transition state **36-TS**, in which the C(11)–C(22) bond between phenyl and ethylene is shortened by 0.48 Å and the C(21)–C(22) bond of ethylene is lengthened by 0.03

Å; the energy slightly increases to 1.19 kcal/mol. The intermediate formed (**37**) has C(11)–C(22) and C(21)–C(22) single bonds and an agostic C–H bond to Pd (Pd(1)–H(25), 1.827 Å and C(22)–H(25), 1.198 Å), at an energy of -17.41 kcal/mol.

The  $\beta$ -H transfer/olefin elimination proceeds through transition state **38-TS** with an energy increase to -9.16 kcal/mol. The Pd(1)–H(25) bond distance shortens to 1.556 Å and the C(22)–H(25) bond distance lengthens to 1.651 Å. Then, the reaction continues to the intermediate  $\text{Pd}(\text{Br})(\text{H})(\text{C}_2\text{H}_3\text{Ph})$  **39** (-20.14 kcal/mol), in which the C(21)–C(22) bond of styrene lies perpendicular to the Br(10)–Pd(1)–H(25) plane opposite the bromide ion, while hydrogen H(25) is cis to bromide ion. Because the product of styrene dissociation,  $\text{Pd}(\text{Br})(\text{H})$  **40**, has no  $\pi$ -acceptor ligands to stabilize the palladium atom, the

**Figure 5.** Molecular structures in the migratory insertion,  $\beta$ -H transfer/olefin elimination, and catalyst recovery of palladium with bromide ion complex. Calculated bond distances and angles are given in Å and deg.

**Scheme 5. Probable Mechanism of the “Ligand-Free” Heck Reaction**

dissociation free energy of styrene is endergonic by 16.59 kcal/mol relative to **39**. Following styrene loss, the base  $\text{NEt}_3$  abstracts the proton H(25) and forms  $\text{Pd}(\text{Br})(\text{H}-\text{NEt}_3)$  **59**, which releases  $\text{HNEt}_3^+$  and  $\text{Br}^-$ ; the formation of the  $\text{Pd}_4$  cluster completes the cycle.

**(5.2) Bromide-Bound Palladium Complex.** On the basis of experimental evidence, de Vries proposed a mechanism in which the halide anion stabilizes atomic palladium and serves as a ligand for palladium catalyst in the “ligand-free” Heck reaction cycle.<sup>4</sup> Although the bromide ion can serve as a spectator ligand like phosphine, it is a  $\pi$ -donor, not a  $\pi$ -acceptor. Because of this lack of  $\pi$ -back-bonding,  $\text{Br}^-$  is not as effective in stabilizing a Pd atom and the energy of  $\text{PdBr}^-$  is relatively high in comparison to  $\text{Pd}(\eta^2\text{-C}_2\text{H}_4)$  and  $\text{PdPR}_3$ .

After the oxidative-addition step,  $[\text{Pd}(\text{Br})(\text{Br})(\text{Ph})]^-$  (**63**) binds ethylene and forms  $[\text{Pd}(\text{Br})(\text{Br})(\text{Ph})(\text{C}_2\text{H}_4)]^-$  (**64**) with a small energy increase from  $-15.88$  (**63**) to  $-11.90$  (**64**) kcal/mol (Scheme 4 and Table 5). The lowest energy isomer has ethylene perpendicular to the coordination plane and cis to the phenyl group (Figure 5); no minima were found for an isomer with ethylene lying in the coordination plane.

Migratory insertion through transition state **65-TS** causes an energy increase to 5.14 kcal/mol. The higher energy barrier for the migratory insertion for **64** compared to that for  $\text{Pd}(\text{Br})(\text{Ph})(\text{C}_2\text{H}_4)$  (**35b**) arises because the ethylene in **35b** is already parallel to the coordination plane. Formation of the intermediate  $[\text{Pd}(\text{Br})(\text{Br})(\text{HC}_2\text{H}_3\text{Ph})]^-$  **66** proceeds with an energy of  $-26.13$  kcal/mol. Interestingly, there is no agostic C–H bond interaction to palladium in the intermediate **66**, unlike the corresponding one with phosphine ligand or ethylene as the supporting ligand.

Then, the hydrogen H(25) transfers to palladium via the transition state **67-TS** ( $-14.10$  kcal/mol) and forms intermediate  $[\text{Pd}(\text{Br})(\text{Br})(\text{H})(\text{C}_2\text{H}_3\text{Ph})]^-$  **68** ( $-17.59$  kcal/mol). The two Pd–Br bonds are in a cis position and the Pd(1)–H(25) bond distance is shortened to 1.548 Å. Finally, the styrene dissociation to form  $[\text{Pd}(\text{Br})(\text{Br})(\text{H})]^-$  **69** is exergonic by  $-10.68$  kcal/mol relative to **68**. The two Pd–Br bonds rearrange to be trans to each other and the Pd(1)–H(25) bond distance shortens further to 1.502 Å. Again, the  $\text{NEt}_3$  base abstracts the proton and forms

intermediate  $[\text{Pd}(\text{Br})(\text{Br})(\text{H}-\text{NEt}_3)]^-$  **70**, which can either lose  $\text{HNEt}_3^+$  and all  $\text{Br}^-$  ions or transiently form  $\text{PdBr}^-$ , then lose  $\text{Br}^-$  and form  $\text{Pd}_4$  to complete the catalytic cycle.

### (5.3) Probable Pathway for Substrate-Bound Palladium.

The free energy profiles for the complete pathways of the Heck reaction with substrate-bound ( $\text{C}_2\text{H}_4$  and  $\text{Br}^-$ ) palladium catalyst are compared in Scheme 4. Although de Vries<sup>4</sup> proposed a mechanism for a “ligand-free” Heck reaction, in which halide ion(s) stabilize the atomic palladium and act(s) as a ligand in the Heck catalytic cycle, our results show that the ethylene substrate is a better ligand than bromide ion to stabilize atomic palladium and abstract it from a palladium cluster. Moreover,  $\text{Pd}(\eta^2\text{-C}_2\text{H}_2)$  leads to lower energy barriers than  $\text{PdBr}^-$  for the oxidative-addition and migratory insertion steps (**34-TS** to **62-TS** and **36-TS** to **65-TS**). However, after the C–C bond formation, the  $\beta$ -H transfer/olefin elimination has a lower barrier for the  $\text{PdBr}^-$  complex (**38-TS** to **67-TS**). In fact, the two pathways can intercross by the association and dissociation of bromide ion. Therefore, the most probable pathway for the so-called “ligand-free” Heck reaction (Scheme 5) begins with the ethylene stabilizing palladium and abstracting Pd atoms from nanoclusters. Then, phenyl bromide binds and the reaction proceeds through the oxidative addition and migratory insertion. Next the bromide ion binds to  $\text{Pd}(\text{Br})(\text{HC}_2\text{H}_3\text{Ph})$  **37** to stabilize this low-coordinated palladium complex and forms  $[\text{Pd}(\text{Br})(\text{Br})(\text{HC}_2\text{H}_3\text{Ph})]^-$  **66** before proceeding with the rest of the reaction. Note that a second ethylene could also take the place of the second bromide, to stabilize the low-coordinated palladium **37**.

## Conclusions

Both phosphine and ethylene can stabilize atomic palladium dissociated from the model nanocluster  $\text{Pd}_4$ . Under conditions with phosphine ligands, monopalladium monophosphine not only plays a role as an active catalyst but can also dimerize to form dipalladium diphosphine (other monopalladium complexes might also undergo this reaction). For large sterically demanding phosphines, such as  $\text{P}^t\text{Bu}_3$ , the phenyl bromide oxidative-addition barrier is lower on monopalladium monophosphine. On the other hand, for the small phosphine ligand, such as  $\text{PMe}_3$  and possibly sterically less demanding phosphines not studied here, the phenyl bromide oxidative addition can proceed more easily via dipalladium diphosphine. Thus, the dipalladium complexes may lead to higher activity and lower energy barriers relative to monopalladium monophosphine. Our results confirm that pathways containing dipalladium species can form viable alternative Heck reaction pathways.

In the absence of phosphine ligand, the substrate-bound palladium complexes were investigated as the potential intermediates for the Heck reaction. The phenyl bromide oxidative addition on  $\text{Pd}(\eta^2\text{-C}_2\text{H}_4)$  has the lowest energy barrier in comparison to  $\text{PdBr}^-$  and bare Pd. Our study concludes that at the beginning of the Heck reaction, the ethylene but not  $\text{Br}^-$  stabilizes atomic palladium well enough to remove an atom from a palladium cluster. Then, phenyl bromide binds and undergoes oxidative addition and migratory insertion. After C–C bond coupling, the binding of an additional bromide ion to low-coordinated  $\text{Pd}(\text{Br})(\text{HC}_2\text{H}_3\text{Ph})$  **37** complex creates a more stable intermediate  $[\text{Pd}(\text{Br})(\text{Br})(\text{HC}_2\text{H}_3\text{Ph})]^-$  **66**, which proceeds through the  $\beta$ -hydride transfer/olefin elimination and catalyst recovery steps over lower barriers. Thus, under phosphine-free condi-

tions, our study reveals additional supporting roles for both ethylene and bromide ion in the Heck reaction. Ethylene acts best as a ligand to stabilize palladium through the oxidative-addition and migratory insertion steps; then the additional ligand, such as a second bromide or perhaps a second ethylene, ligates to the open site to stabilize the low-coordinated palladium complex before releasing the styrene product and recovering the active palladium catalyst.

**Acknowledgment.** We would like to thank the National Science Foundation (Grant Nos. CHE-0518074, CHE-0541587, and DMS-0216275), the Welch Foundation

(Grant No. A-0648), and Royal Thai Government for financial support.

**Supporting Information Available:** Details related to standard state conversion, molecular structures in the Heck catalytic cycle for the monopalladium complex with the  $\text{PMe}_3$  ligand, and selected geometry parameters for all computed intermediate species. This material is available free of charge via the Internet at <http://pubs.acs.org>.

OM800787Y